HHS Public Access

Author manuscript

J Mol Cell Cardiol. Author manuscript; available in PMC 2020 March 11.

Published in final edited form as:

J Mol Cell Cardiol. 2019 June ; 131: 53–65. doi:10.1016/j.yjmcc.2019.04.016.

The role of fibroblast – Cardiomyocyte interaction for atrial dysfunction in HFpEF and hypertensive heart disease

David Bode[a,b,e], **Diana Lindner**[c,d], **Michael Schwarzl**[c,d], **Dirk Westermann**[c,d], **Peter Deissler**[a,b], **Uwe Primessnig**[a,b,e], **Niklas Hegemann**[a,b], **Lothar A. Blatter**[f], **Sophie van Linthout**[a,b], **Carsten Tschöpe**[a,b], **Felix Schoenrath**[b,g], **Sajjad Soltani**[b,g], **Christof Stamm**[b,g], **Volker Duesterhoeft**[b,g], **Natale Rolim**[j], **Ulrik Wisløff**[j], **Christoph Knosalla**[b,g], **Volkmar Falk**[b,g,h], **Burkert M. Pieske**[a,b,e,i], **Frank R. Heinzel**[a,b], **Felix Hohendanner**[a,b,e,*]

[a]Department of Internal Medicine and Cardiology, Charité – Universitätsmedizin Berlin, Campus Virchow-Klinikum, Augustenburgerplatz 1, 13353 Berlin, Germany

[b]DZHK (German Centre for Cardiovascular Research), partner site Berlin, Germany

[c]DZHK (German Centre for Cardiovascular Research), partner site Hamburg, Germany

[d]Universitäres Herzzentrum Hamburg, Klinik für Allgemeine und Interventionelle Kardiologie, 20246 Hamburg, Germany

[e]Berlin Institute of Health (BIH), Berlin, Germany

[f]Department of Physiology and Biophysics, Rush University, Chicago, USA

[g]Department of Cardiothoracic Surgery, German Heart Center Berlin, Augustenburgerplatz 1, 13353 Berlin, Germany

[h]Department of Cardiothoracic Surgery, Charité – Universitätsmedizin Berlin, corporate member of Freie Universität Berlin, Humboldt-Universität zu Berlin and Berlin Institute of Health, Germany

[i]Department of Internal Medicine and Cardiology, German Heart Center Berlin, 13353 Berlin, Germany

[j]K.G. Jebsen Center of Exercise in Medicine, Department of Circulation and Medical Imaging, Norwegian University of Science and Technology (NTNU), Trondheim, Norway.

Abstract

Aims—Atrial contractile dysfunction is associated with increased mortality in heart failure (HF). We have shown previously that a metabolic syndrome-based model of HFpEF and a model of hypertensive heart disease (HHD) have impaired left atrial (LA) function in vivo (rat). In this study we postulate, that left atrial cardiomyocyte (CM) and cardiac fibroblast (CF) paracrine interaction related to the inositol 1,4,5-trisphosphate signalling cascade is pivotal for the manifestation of

*Corresponding author at: Department of Internal Medicine and Cardiology, Charité University Medicine, CVK, Augustenburger Platz 1, 13353 Berlin, Germany, *address:* felix.hohendanner@charite.de (F. Hohendanner).

Conflicts of interest

Conflicts of Interest: none declared.

Appendix A. Supplementary data

Supplementary data to this article can be found online at https://doi.org/10.1016/j.yjmcc.2019.04.016

atrial mechanical dysfunction in HF and that quantitative atrial remodeling is highly disease-dependent.

Methods and results—Differential remodeling was observed in HHD and HFpEF as indicated by an increase of atrial size in vivo (HFpEF), unchanged fibrosis (HHD and HFpEF) and a decrease of CM size (HHD). Baseline contractile performance of rat CM in vitro was enhanced in HFpEF. Upon treatment with conditioned medium from their respective stretched CF (CM-SF), CM (at 21 weeks) of WT showed increased Ca^{2+} transient (CaT) amplitudes related to the paracrine activity of the inotrope endothelin (ET-1) and inositol 1,4,5-trisphosphate induced Ca^{2+} release. Concentration of ET-1 was increased in CM-SF and atrial tissue from WT as compared to HHD and HFpEF. In HHD, CM-SF had no relevant effect on CaT kinetics. However, in HFpEF, CM-SF increased diastolic Ca^{2+} and slowed Ca^{2+} removal, potentially contributing to an in-vivo decompensation. During disease progression (i.e. at 27 weeks), HFpEF displayed dysfunctional excitation-contraction-coupling (ECC) due to lower sarcoplasmic-reticulum Ca^{2+} content unrelated to CF-CM interaction or ET-1, but associated with enhanced nuclear [Ca^{2+}]. In human patients, tissue ET-1 was not related to the presence of arterial hypertension or obesity.

Conclusions—Atrial remodeling is a complex entity that is highly disease and stage dependent. The activity of fibrosis related to paracrine interaction (e.g. ET-1) might contribute to in vitro and in vivo atrial dysfunction. However, during later stages of disease, ECC is impaired unrelated to CF.

Keywords

Atrial remodeling; HFpEF; Cardiac fibroblasts; Atrial cardiomyocyte; Excitation-contraction coupling

1. Introduction

Heart failure (HF) with preserved ejection fraction (HFpEF) represents a clinical syndrome with patients suffering from typical symptoms of HF, while showing a normal left-ventricular ejection fraction (LVEF; ≥50%) [1]. HFpEF accounts for 40–71% of HF patients. While pharmacological treatment significantly improved clinical outcomes of patients with systolic heart failure (HFrEF), the prognosis for patients suffering from HFpEF has remained unchanged [2]. Metabolic syndrome has been associated with diastolic dysfunction and identified as an independent predictor of new-onset HFpEF [3].

Left atrial (LA) remodeling is a hallmark feature of HFpEF and other cardiac diseases (e.g. hypertensive heart disease (HHD)) and commonly associated with LA enlargement and dysfunction. LA remodeling is a predictor of new-onset HF [4] and atrial fibrillation (AF), while reduction in LA ejection fraction (LA-EF) is an independent predictor of mortality [5]. Growing insight into the key role of atrial function in cardiac disease has recently given rise to the concept of ‘atrial cardiomyopathies’ [6]. While highly prevalent, the quantification of different stages of atrial remodeling during HF and preceding conditions as well as the underlying mechanisms remain elusive.

Pathological hypertrophy and interstitial fibrosis are hallmarks of HF. Increased fibrosis per se is an important contributor to mechanical and electrical dysfunction as fibroblasts do not

contribute to contractile function and affect electrical propagation. However, fibrosis might influence neighboring CM also directly via paracrine mediators. Recently we have identified neurohumoral activation, involving the renin-angiotensin-aldosterone-system (RAAS) as a potential contributor to contractile dysfunction in HFpEF-related LA remodeling [7]. Beside the RAAS, myocardial inflammation and a pro-fibrotic environment are pivotal triggers of adverse myocardial remodeling and may pose interesting targets for the development of drug therapies [8]. In cardiac tissue, paracrine mediators play an integral part in intercellular communication and have been shown to mediate interstitial myocardial fibrosis [9,10]. In turn, activated cardiac fibroblasts (CF) have been shown to contribute to myocardial inflammation in patients with HFpEF [11]. Experimental studies suggest, that CF-derived mediators are capable of directly altering CM function via regulation of gap junctions and ion channel expression [12].

We postulate, that the interaction between CM and CF via CF-derived mediators is pivotal for atrial in vivo and in vitro dysfunction in HFpEF, as well as in HHD. We also postulate that independent of fibrosis quantity, its “activity” significantly influences atrial function. We further investigated paracrine mediators like ET-1 and their relevance for atrial function in this context. At the same time, we seek to provide evidence that differential cellular and in vivo remodeling can be observed during different stages of HHD and HFpEF. The present data helps to establish a crucial role for direct cellular CM – CF interaction in several clinically highly relevant settings of atrial dysfunction (i.e. hypertensive heart disease and HFpEF). In a translational approach, we also investigated an association of a CF-derived mediator (i.e. atrial tissue ET-1) and the presence of particular co-morbidities (i.e. arterial hypertension, obesity) in humans.

2. Methods

The investigation conforms to the *Guide for the Care and Use of Laboratory Animals* published by the US National Institutes of Health (NIH Publication No. 85–23, revised 1985) and the principles outlined in the *Declaration of Helsinki* (*Br Med J* 1964; ii: 177).

2.1. Patient data

All patients gave written informed consent to participate in the study (DZHK Biobank, German Heart Center Berlin). Excess patient tissue was obtained from right atria during routine surgery and clinical data (presence of overt arterial hypertension, i.e. systolic blood pressure > 139 mmHg; obesity, i.e. body mass index > 25 kg/m^2) was gathered from existing in-hospital documentation.

2.2. Animal echocardiography

Echocardiography was performed as previously described [13]. In brief, rats were anesthetized and transthoracic echocardiography performed with a high-resolution micro-imaging system equipped with a 17.5-Mhz linear array transducer (Vevo770TM Imaging System, VisualSonics, USA) using standard 2D imaging. Measurements were performed to assess changes in LA dimensions (LA size) from at least three consecutive cardiac cycles under stable conditions.

2.3. HF model

Animal experiments were approved by local authorities (G0276/16). The well characterized ZFS-1 HF rat model is based on a leptin receptor mutation leading to a lean (heterozygous; arterial hypertension) and obese (homozygous; metabolic syndrome, HFpEF) phenotype [14]. WT, HHD and HFpEF animals were fed a high caloric diet (Formulab Diet 5008). LA CM were isolated from 21-week-old ZSF-1 lean (HHD; $ZSF^{+/-}$), ZFS-1 obese (HFpEF; $ZSF^{+/+}$) and wild type (WT; Wistar Kyoto; Charles River) and after disease progression at 27–28 weeks from HFpEF (still without systolic dysfunction [15]) and WT as previously described [13]. WT animals (CTRL; Wistar; Charles River) for in-vitro experiments with bosentan and 2-APB were fed standard diet for 21 weeks.

2.4. CM isolation

Animals were anesthetized with isoflurane and euthanized by cervical dislocation. The heart was excised, mounted on a Langendorff-apparatus and perfused with nominally Calcium (Ca^{2+})-free Tyrode solution for 3 min, followed by enzyme solution containing 0.035 Wünsch units/ml Liberase TM and 10 μM Ca^{2+}. The LA was separated from the heart, minced, filtered and washed. Isolated cells were stepwise adjusted to Tyrode solution containing 1 mM Ca^{2+} and kept at room temperature until subsequent experimentation.

2.5. ELISA

ELISAs were performed according to the manufacturers' protocol (R&D Systems, Minneapolis, MN: IL-1β, IL-6, IL-10, IL-33, PDGF, TGF-β, TNF-α; Enzo Life Sciences, Lausen, Switzerland: ET-1).

2.6. Histologic analysis

Hearts were excised after euthanasia, washed in phosphate-buffered-saline and the LA separated from the remaining organ. Tissue specimen were fixed and paraffin-embedded. Histologic slides were stained with Picrosirius Red (Morphisto, Frankfurt am Main, Germany) in order to assess cardiac fibrosis.

Interstitial myocardial fibrosis was defined as the percentage fraction of Picrosirius Red-stained collagen fibers from the total image. Endo- and epicardial fibrotic tissue was manually excluded by a blinded expert in veterinary pathology. Interstitial myocardial fibrosis was automatically assessed and calculated using ImageJ (National Institutes of Health, Bethesda, MD; ImageJ Macro attached in Supplement).

2.7. Solution and chemicals

Chemicals were obtained from Sigma-Aldrich (St. Louis, MO, USA) unless noted otherwise. Fluorescent Ca^{2+} indicators Fluo-4 AM and Fura-2 AM were obtained from Thermo Fisher Scientific (Waltham, MA, USA). Tyrode solution contained (in mM): 130 NaCl, 4 KCl, 2 CaCl, 1 $MgCl_2$, 10 Glucose, 10 HEPES; pH adjusted to 7.4 with NaOH. Cells were plated on laminin-coated glass coverslips. For experiments with condition medium derived from CF, the respective medium was diluted 1:1 with Tyrode solution and cells incubated for 1 h at 37 °C. The endothelin receptor blocker Bosentan and the

inositol-1,4,5-trisphosphate (IP_3)-receptor blocker 2-Aminoethoxydiphenyl borate (2-APB) were used at a concentration of 100 and 10 μM, respectively.

2.8. Cell culture

The hearts from 21-week-old rats were used to obtain primary CF from LA tissue as described previously [16]. LA tissue was used from a total of 4 animals/group for the subsequent steps. After separation of atria and ventricle, tissue was digested in 0.1 mg/ml Liberase (Roche, Germany) dissolved in Hanks' Balanced Salt Solution while gently shaking at 37 °C for 10 min. The supernatant containing the isolated cells was collected and immediately placed on ice. The remaining tissue was used for an additional digestion cycle. This tissue digestion was repeated six times consecutively. Cells were separated through a cell strainer and enzymatic solution was removed after centrifugation. Cells were collected in complete growth medium (Dulbecco's Modified Eagle Medium (DMEM)) containing 20% fetal calf serum (FCS), 100 U/ml penicillin and 100 μg/ml streptomycin and seeded in cell culture flask. For sub-culturing, cells were detached utilizing trypsin/EDTA solution. To mechanically activate CF, cells were placed on collagen-I coated flexible-bottomed 6-well culture plates (Bioflex plates, Dunn). Mechanical stretch was applied using the Flexercell System FX-4000 Tension Plus (Dunn) to deform the cultured cells using an elongation of 10% at a frequency of 1 Hz. Prior to mechanical stretch, cells were starved overnight in serum reduced medium (DMEM containing 0.5% FCS, 100 U/ml penicillin and 100 μg/ml streptomycin. The mechanical stimulation was performed in the presence of a protease inhibitor cocktail (P1860) for 3 h to investigate gene expression analysis or for 72 h to produce the cell culture supernatant for subsequent cellular experiments.

2.9. Confocal and ratiometric Ca^{2+} measurements

For confocal Ca^{2+} measurements, cells were loaded with Fluo-4 AM as previously described [7]. Transversal or longitudinal confocal line scan images were recorded at 1250 lines per second using a 40 × oil-immersion objective lens (NA: 1.49; pixel size 0.12 μm) with a Zeiss LSM 800 system. Ca^{2+} transients (CaT) were elicited by electrical field stimulation (frequency: 1 Hz) of intact LA CM with a pair of platinum electrodes (voltage: ~50% above contractile threshold). Changes in Ca^{2+} are expressed as the amplitude $\Delta F/F_0$, where F represents time-dependent Fluo-4 fluorescence, F_0 represents diastolic fluorescence levels under steady-state conditions during electrical stimulation and $\Delta F = F - F_0$. Tau of a mono-exponential fit of the decay of CaT was obtained as a parameter of Ca^{2+} removal. At 27-weeks, a subset of cells was exposed to Tyrode solution containing caffeine (20 mM) and the subsequent Ca^{2+} release, expressed as $\Delta F/F_0$, taken as a measure of Ca^{2+} content of the sarcoplasmic reticulum (SR).

For ratiometric Ca^{2+} measurements, cells were loaded with Fura-2AM (1 μM; excitation: 340 nm and 380 nm, emission: 510 ± 10 nm) for 30 min at room temperature. Background signals were subtracted and changes of Ca^{2+} are expressed as the ratio $R = F_{340}/F_{380}$.

2.10. Visualization of global cell shortening

For measurements of contractility cell shortening along the longitudinal axis during 1 Hz electrical stimulation was measured with video edge detection (time resolution: 60 frames/s;

PTI FelixGX, HORIBA Scientific, Edison, NJ). Cell shortening is expressed as the change in systolic relative to diastolic cell length. Tau of a mono-exponential fit of the decay of contraction traces was obtained as a parameter of cell relaxation.

2.11. Data analysis and statistics

Data were analyzed as previously described [3]. Results are shown as mean ± standard error. Statistical analysis was performed by using unpaired Student's *t*-test or analysis of variance for multiple comparisons, followed by the Bonferroni post-hoc test. A two-tailed p value of < 0.05 was used to indicate statistical significance.

3. Results

3.1. LA remodeling in HFpEF and HHD is not related to the degree of fibrosis

LA fibrosis is a hallmark feature of remodeling and LA in vivo function is impaired in HFpEF [7]. However, LA fibrosis was unchanged in HHD at 21 weeks as compared to WT. In HFpEF at 21 weeks, LA interstitial fibrosis was also unchanged compared to WT and HHD (Fig. 1B and C). In order to evaluate the potential contribution of LA fibrosis in advanced disease progression, interstitial fibrosis of HFpEF was evaluated at a later time-point (27 instead of 21 weeks), where again no difference could be observed compared to WT (Fig. 1F).

Similar results were obtained using a semi-quantitative analysis of localized LA fibrosis. Transmural distribution of fibrosis was unchanged (subendocardial, subepicardial, myocardial; Supp. Fig. 1).

3.2. Differential LA remodeling and enhanced in vitro contractile function can be observed in HHD and HFpEF

In addition to the observed unchanged fibrosis, CM size tended to be reduced in HHD (Fig. 2A and B). At the same time, LA diameter was significantly increased in HFpEF vs. HHD and WT, indicating differential LA remodeling (Fig. 2C).

However, in vitro, this was accompanied by a significantly increased cell shortening of LA CM in comparison to WT (Fig. 2D and E). LA CM in HFpEF showed an acceleration of contractile kinetics: Time-to-peak was shorter compared to WT and relaxation (tau) was faster compared to WT and HHD. However, LA CM from HHD showed a significant acceleration in time-to-peak compared to WT, but no significant change of cell shortening amplitude and cell relaxation (Fig. 2F and G). These results further underscore the differential remodeling observed during HHD and HFpEF at 21 weeks.

3.3. Stretched cardiac fibroblasts enhance Ca^{2+} cycling during excitation-contraction coupling in WT (21w)

LA structure and function showed marked differences on the in vivo and in vitro level in WT, HHD and HFpEF. To resolve the conundrum of an enhanced in vitro function, impaired in vivo function, yet unchanged fibrosis, we next investigated the impact of CF – CM interaction on atrial function in the setting of mechanical stretch in the different models.

First, we studied the impact of increased cellular distention as it might occur during conditions of increased preload on WT animals. In order to simulate this condition in vitro, cultured CF from their respective groups were stretched and the conditioned medium collected. Subsequently, isolated LA CM were treated with their respective conditioned medium of unstretched (CM-NSF) or stretched CF (CM-SF) and Ca^{2+} measured ratiometrically. After treatment with CM-NSF, LA CM showed increased diastolic [Ca^{2+}] as compared to control conditions (NT2, Fig. 3B). Interestingly when treated with CM-SF, diastolic [Ca^{2+}] increased even further (Fig. 3B). In addition, CaT amplitudes were significantly increased upon exposure to CM-SF. Similar results were obtained with confocal measurements and a different [Ca^{2+}] sensitive dye (fluo-4, not shown). Confocal measurements were used to differentiate subcellular differences of CaT kinetics: CM-SF led to a faster time-to-peak CaT and faster [Ca^{2+}] removal (i.e. tau was smaller, Fig. 3G and H). The effect was equally strong in subsarcolemmal and central cytosolic compartments of the cells.

3.4. Cardiac fibroblasts alter diastolic Ca^{2+} in HHD (21w)

Next, we repeated these experiments in the HHD animals. Interestingly there was not significant effect on CaT amplitudes or kinetics (Fig. 4C–E), even though diastolic [Ca^{2+}] tended to be increased with CM-NSF as compared to control (NT2, Fig. 4B). In support of this data no difference of amplitude (not shown) or kinetics of CaT were found with confocal [Ca^{2+}] measurements (Fig. 4F–H).

3.5. Stretched cardiac fibroblasts impair LA in vitro function in HFpEF (21w)

LA in HFpEF showed an increased diameter (Fig. 2A), indicating LA remodeling accompanied by increased cellular distention in vivo. Stretch-related changes in the composition of fibroblast medium had significantly different effects on the kinetics of the CaT in CM from HFpEF hearts.

After treatment with CM-SF, LA CM in HFpEF showed significantly increased diastolic Ca^{2+} and a reduced area under the curve for CaT as compared to control. The area under the curve represents a measure of Ca^{2+} exposure of the myofilaments and might therefore correlate with contractility (Fig. 5B and E). As opposed to the previously observed effect in WT, the Ca^{2+} amplitude remained unchanged upon exposure to CM-SF (Fig. 5D). In addition, CM-SF significantly increased tau throughout the cytosol (Fig. 5H), indicating slower cellular relaxation upon exposure to stretched fibroblast media.

3.6. ET-1 and other paracrine mediators are altered in CM-SF and potentially related to the observed functional differences

In order to further explore mechanisms involved in impaired LA function in the animal model, gene expression analysis of cultured CF was performed in search of genomic switches which may contribute to the facilitation of CF-induced ECC dysfunction in LA CM. We found significant changes of IL-6 on the mRNA level upon stretch (Supp. Fig. 2). Additionally, conditioned medium obtained from cultured CF was screened by ELISA for a range of cytokines known to modulate fibrosis and inflammation (Fig. 6). Concentrations of IL-1β, IL-33, PDGF, TGF-β and TNF-α were below detection threshold (< 31.3 or < 12.5

pg/ml, resp. n.s.). However, as shown in Fig. 6A, ET-1 and IL-6 were especially prevalent in WT CM-SF. While HHD media still contained ET-1 and IL-6 upon stress (Fig. 6B), this response was blunted in HFpEF CM-SF (Fig. 6C). In support of this data, tissue ET-1 concentration was significantly reduced in HFpEF (Fig. 6D). ET-1 is known to be a potent inotrope in a variety of animal models: ET-1 augmented sarcoplasmic reticulum Ca^{2+} release (Suppl. Fig. 3) even in the presence of the ryanodine receptor inhibitor tetracaine. When blocking ET-1 receptors in cells exposed to CM-SF, the inotropic response was mitigated and diastolic and systolic [Ca^{2+}] tended to be even decreased. This indicates that ET-1 is a decisive part of the paracrine “cocktail” mediating positive inotropic effects in WT animals upon stretch (Fig. 6E). In support of this notion, application of the IP_3-receptor blocker 2-APB lowered systolic and diastolic Ca^{2+} to control levels (Fig. 6F). Moreover, the lower concentration of ET-1 in HHD and HFpEF tissue as well as in HHD and HFpEF CM-SF indicates an absent additional production of this inotropic substance upon stretch during atrial remodeling.

3.7. Atrial CM dysfunction is related to impaired excitation-contraction coupling during progression of HFpEF (27w) and paralleled by increased nuclear Ca^{2+}

As shown in Fig. 2, baseline LA CM function was preserved or even improved in HHD and HFpEF, while the interaction between CF and CM led to in vitro decompensation (Figs. 4 and 5). Next, we explored atrial remodeling in the setting of disease progression in HHD and HFpEF. With advanced age, LA diameter was still significantly increased in HHD and HFpEF (Fig. 7B), while LA function was preserved in HHD and tended to be reduced in HFpEF (Fig. 7D). Clinically, animals still showed a preserved left ventricular ejection fraction (suppl. Fig. 4D). However, during disease progression (i.e. at 27-weeks) LA CM showed a significant impairment of ECC under baseline conditions. LA CM of HFpEF presented with a lower CaT amplitude, a slower Ca^{2+} removal (almost 2-fold increase of tau) and increased time-to-peak compared to WT (Fig. 7F–H). These observations could be explained by a significant reduction of sarcoplasmic reticulum Ca^{2+} content in HFpEF (Fig. 7I).

An increase of nuclear Ca^{2+} has been associated with cardiac remodeling [17]. Interestingly and in support of this notion, LA CM during later stages of HFpEF had a significantly augmented CaT amplitude during ECC in the nuclear cell compartment (Fig. 7J).

3.8. Stretched cardiac fibroblasts have no adverse effect on Ca^{2+} cycling during excitation-contraction coupling in WT, HHD or HFpEF in disease progression (27w)

We tested if CM-SF had an additional positive or negative effect on CaT amplitudes and kinetics in vitro in WT, HHD and HFpEF, respectively. Upon exposure to CM-SF neither WT cells (Fig. 8A–D), nor HHD (Fig. 8E–H) or HFpEF cells (Fig. 8I–L) showed altered CaT during excitation-contraction coupling. Interestingly at this later disease stage, atrial tissue ET-1 concentration was not significantly different between WT, HHD and HFpEF (Fig. 8M). This supports the notion that atrial enlargement as observed in vivo led to no further increase of fibroblasts ET-1 secretion at 27 weeks. However, ET-1 concentration within the particular groups still positively affected left atrial ejection fraction (Fig. 8N) which is in agreement with the presented results in Figs. 3–5. Last, we tested the hypothesis

that tissue ET-1 concentration differed between in humans with arterial hypertension or diastolic dysfunction. Human myocardial ET-1 was quantified by ELISA from a total of 16 patients. However, as compared to control patients, atrial tissue ET-1 was not significantly altered (Fig. 8O).

4. Discussion

Atrial remodeling has been shown to affect morbidity and mortality of patients and recent results from clinical studies like CASTLE-AF suggest that altering the course of atrial cardiomyopathy (with its signature feature atrial fibrillation) positively influences survival [18]. Several disease entities like hypertension or heart failure are associated with atrial remodeling, which is thought to be related to impaired cardiomyocyte function and altered fibrosis [19]. However, even though clinically highly relevant, the exact mechanism of differential atrial cardiomyopathies are not well understood. We therefore investigated the interaction between the most prevalent cell types in atria that contribute to remodeling, cardiomyocytes and fibroblasts, in different disease states and entities. Here, we show for the first time, that an altered “activity of fibrosis”, independent of the extent of fibrotic remodeling, affects atrial function in the context of healthy and diseased hearts in a time-dependent manner.

Quantitative differences of fibrosis directly influence atrial contractility in the setting of atrial cardiomyopathy [20,21]. In addition, local differences of fibrosis with potentially pro-arrhythmic and deteriorating effects regarding tissue mechanics have been shown to be especially prevalent in obesity related atrial remodeling [19]. Interestingly however, in our animal model, fibrosis was quantitatively not altered, even though atria were enlarged and atrial function was impaired [7]. This is in line with data presented e.g. by Khan et al. who found no difference in total collagen content in atria of a canine model of heart failure [22]. A setting that allowed us to study the impact of the “activity of fibrosis” on atrial function in HHD and HFpEF in detail.

An interaction between CF and CM and vice-versa leading to altered function has been proposed in the past, yet evidence was lacking [23]. Our data indicates that stretch of CF presents as an important trigger for the activation of fibrosis and changes the paracrine signature of fibroblasts, with differential effects on “neighboring” cardiomyocytes. Indeed, stretch has been shown to activate a plethora of different cell types to augment or alter their function [11]. Our data shows an increase in IL-6 expression mirroring this cellular activation through stretch.

ET-1 is a potent inotrope [24] that allows to even overcome impaired Ca^{2+} release through ryanodine receptors most likely via its activation of inositol-1,4,5-phosphate receptors [25]. ET-1 release has been linked to mechanical stress [26]. It can also foster remodeling processes like enhanced fibrosis and hypertrophy with prolonged exposure [27]. In the studied healthy WT rats, stretched fibroblasts secreted high concentrations of ET-1 which led to an IP_3-receptor dependent augmentation of CM function. IP_3R mediated Ca^{2+} release has been shown to be highly important in atrial cells and to allow compensatory augmentation of contractility [28]. Indeed, tissue ET-1 concentrations positively correlated

with left atrial function in our animal model. In vivo, fibroblast ET-1 release upon stretch and its impact on CM function might therefore very well represent a compensatory mechanism to account for increased hemodynamic demands.

Stretch however has been shown to also have opposite effects, especially in the context of cardiac disease. Chronic overload as occurring during HF has been associated with impaired ECC in CM [29]. In addition, pro-fibrotic signalling cascades and cytokines, known to modulate CF activity and enhance remodeling, are activated through stretch in this setting [30]. CF activity itself is altered through stretch [31]. In support of this notion, Ca^{2+} cycling during ECC was impaired in early stage HFpEF due to an altered composition of CF secretions, potentially contributing to the observed in vivo phenotype of an impaired atrial contractility [7]. Various cytokines and paracrine mediators that are excreted by CF have been associated with a potential impairment of contractile function [32]. Even though we found no detectable change in IL-1β, IL-6, IL-10, IL-33, PDGF, TGF-β or TNF-α in the supernatant in the animal model, it is likely that a cytokine “cocktail” has potentiating possibly adverse effects on tissue mechanics [33].

During disease progression in our animal model and in human patients, we found no association between tissue ET-1 concentrations and arterial hypertension or obesity, further challenging the relevance of ET-1 as the sole mediator for the observed effects of mechanically stressed atrial fibroblasts on atrial function during particular states of remodeling. Even though plasma levels of ET-1 have been shown to be elevated in HFrEF patients [34], previous studies have failed to correlate myocardial ET-1 with LA remodeling in the absence of AF [35] in humans, corroborating our results.

Interestingly, in early stage and progressive hypertensive heart disease the CF – CM interaction was of less importance regarding cellular function. LA diameter was unchanged as compared to WT and significantly smaller than in HFpEF. In addition, CM size tended to be decreased. At the same time, the extent of fibrosis was unchanged. These morphological findings indicate an earlier but also differential state of remodeling. Others described similar findings in early stage heart failure, where total collagen was unchanged and gelatinase and metalloprotease activity influencing “dynamic collagen turnover” was increased [22]. In HHD, CM-SF, showing smaller yet relevant concentrations of ET-1 and IL-6 as compared to WT, significantly increased diastolic Ca^{2+}, indicating a less pronounced activation of CF upon stress and a less pronounced susceptibility of CM towards CM-SF. In progressive HHD (27w), LA were significantly enlarged, yet left atrial function was unimpaired. As opposed to the great impact of CM-SF on HFpEF (21w), in progressive HHD (27w) CM-SF had no effect on ECC, again underscoring differences in cellular remodeling. Others have shown that atrial enlargement occurs in rats with a comparable genetic background at older ages of up to 25 months and that LA myocytes eventually show impaired baseline ECC during further disease progression [36]. Moreover, in progressive HHD, left ventricular function was preserved indicating that atrial macroscopic remodeling can be observed even before ventricular changes become apparent. Similar findings have been reported in larger animal models by others [37].

In advanced HFpEF, contractile function was even impaired without exposure to CF derived factors. This could be related to decreased sarcoplasmic reticulum Ca^{2+} content and therefore altered ECC per se [38], possibly due to a maximal *baseline* activation of IP_3Rs. The fact that CM-SF had no additional effect on ECC in advanced HFpEF is in agreement with earlier results from HF rabbits, where increased *baseline* activation of the IP_3R signalling cascade itself could be shown to contribute to the Ca^{2+} related atrial contractile dysfunction [28].

The variety of mechanisms leading to atrial mechanical dysfunction at different stages and with different underlying causes of disease is underscored by findings from Yeh et al.: The group has even found enhanced Ca^{2+} release in combination with impaired cellular contractility in atrial remodeling caused by congestive heart failure. They reported that this was related to altered phosphorylation states of myosin-binding protein C rather than Ca^{2+} release itself. Others have associated progressive remodeling processes with altered nuclear $[Ca^{2+}]$ [17]. Interestingly and in support of this concept, in our older animals, nuclear Ca^{2+} release was enhanced.

In summary, we show an interaction between stressed CF and CM, potentially representing a compensatory mechanism in healthy atria, that might contribute to in vivo atrial dysfunction in the setting of HFpEF. We identified ET-1 as a contributor to enhanced left atrial ejection fraction and cellular contractility under normal conditions, but with adverse effects in HFpEF. However, we also found CF - CM interactions to be highly stage and underlying-disease dependent, as Ca^{2+} release was impaired independently of CF during progression of HFpEF. In support of this, CF had no effect on atria in hypertensive remodeling and ET-1 tissue concentrations were unaltered in human arterial hypertension or obesity. Our findings underscore the complex mechanisms underlying atrial remodeling and establish the “activity of fibrosis” related to paracrine interaction with CM (e.g. via ET-1) as an important stage-dependent contributor to in vitro and in vivo atrial dysfunction.

Supplementary Material

Refer to Web version on PubMed Central for supplementary material.

Acknowledgements

The authors thank Mareile Schröder for technical assistance.

Funding

This work was supported by the German Society of Cardiology, the Else-Kröner-Fresenius Stiftung, the DZHK (German Centre for Cardiovascular Research) and by the BMBF (German Ministry of Education and Research) (F.H.). D.B. is an MD stipend of the Berlin Institute of Health. Dr. Hohendanner is participant in the BIH-Charité Clinical Scientist Program funded by the Charité –Universitätsmedizin Berlin and the Berlin Institute of Health. L.A.B. was supported by National Institute of Health grants HL057832, HL132871 and HL134781.

List of abbreviations

AF	atrial fibrillation
Bos	Bosentan

CaT	Calcium transient
Ca^{2+}	Calcium
CM	cardiomyocyte
CM-SF	conditioned medium from stretched cardiac fibroblasts
CM-NSF	conditioned medium from non-stretched cardiac fibroblasts
CF	cardiac fibroblast
ECC	excitation-contraction-coupling
ET-1	Endothelin-1
HF	heart failure
HHD	hypertensive heart disease
HFpEF	heart failure with preserved ejection fraction
HFrEF	heart failure with reduced ejection fraction
IL	Interleukin
IP_3	inositol 1,4,5-trisphosphate
LA	left atrium
LA-EF	left atrial ejection fraction
PDGF	Platelet-derived growth factor
RAAS	renin-angiotensin-aldosterone-system
SR	sarcoplasmic reticulum
TGF	Transforming growth factor
TNF	Tumor necrosis factor
WT	Wildtype
2-APB	2-Aminoethoxydiphenyl borate

References

[1]. Ponikowski P, et al., ESC guidelines for the diagnosis and treatment of acute and chronic heart failure: the task force for the diagnosis and treatment of acute and chronic heart failure of the European Society of Cardiology (ESC). Developed with the special contribution of the heart failure association (HFA) of the ESC, Eur. J. Heart Fail 18 (8) (2016) 891–975. [PubMed: 27207191]

[2]. Owan TE, et al., Trends in prevalence and outcome of heart failure with preserved ejection fraction, N. Engl. J. Med 355 (3) (2006) 251–259. [PubMed: 16855265]

[3]. Hohendanner F, et al., Intracellular dyssynchrony of diastolic cytosolic [ca(2)(+)] decay in ventricular cardiomyocytes in cardiac remodeling and human heart failure, Circ. Res 113 (5) (2013) 527–538. [PubMed: 23825358]

[4]. Habibi M, et al., Association of CMR-measured LA function with heart failure development: results from the MESA study, JACC Cardiovasc. Imaging 7 (6) (2014) 570–579. [PubMed: 24813967]

[5]. Gupta S, et al., Left atrial structure and function and clinical outcomes in the general population, Eur. Heart J 34 (4) (2013) 278–285. [PubMed: 22782941]

[6]. Goette A, et al., EHRA/HRS/APHRS/SOLAECE expert consensus on atrial cardiomyopathies: definition, characterisation, and clinical implication, J Arrhythm 32 (4) (2016) 247–278. [PubMed: 27588148]

[7]. Hohendanner F, et al., Cellular mechanisms of metabolic syndrome-related atrial decompensation in a rat model of HFpEF, J. Mol. Cell. Cardiol 115 (2018) 10–19. [PubMed: 29289652]

[8]. Heymans S, et al., Inflammation as a therapeutic target in heart failure? A scientific statement from the translational research Committee of the Heart Failure Association of the European Society of Cardiology, Eur. J. Heart Fail 11 (2) (2009) 119–129. [PubMed: 19168509]

[9]. Esposito G, et al., Sitagliptin reduces inflammation, fibrosis and preserves diastolic function in a rat model of heart failure with preserved ejection fraction, Br. J. Pharmacol 174 (22) (2017) 4070–4086. [PubMed: 27922176]

[10]. Takeda N, et al., Cardiac fibroblasts are essential for the adaptive response of the murine heart to pressure overload, J. Clin. Invest 120 (1) (2010) 254–265. [PubMed: 20038803]

[11]. Lindner D, et al., Cardiac fibroblasts support cardiac inflammation in heart failure, Basic Res. Cardiol 109 (5) (2014) 428. [PubMed: 25086637]

[12]. Vasquez C, et al., Enhanced fibroblast-myocyte interactions in response to cardiac injury, Circ. Res 107 (8) (2010) 1011–1020. [PubMed: 20705922]

[13]. Bode D, et al., Isolation of atrial cardiomyocytes from a rat model of metabolic syndrome-related heart failure with preserved ejection fraction, J. Vis. Exp (137) (2018).

[14]. Hamdani N, et al., Myocardial titin hypophosphorylation importantly contributes to heart failure with preserved ejection fraction in a rat metabolic risk model, Circ. Heart Fail 6 (6) (2013) 1239–1249. [PubMed: 24014826]

[15]. Bowen TS, et al., Exercise training reveals inflexibility of the diaphragm in an animal model of patients with obesity-driven heart failure with a preserved ejection fraction, J. Am. Heart Assoc 6 (10) (2017).

[16]. Hinrichs S, et al., Precursor proadrenomedullin influences cardiomyocyte survival and local inflammation related to myocardial infarction, Proc. Natl. Acad. Sci. U. S. A. 115 (37) (2018) E8727–E8736. [PubMed: 30166452]

[17]. Ljubojevic S, et al., Early remodeling of perinuclear Ca2+ stores and nucleoplasmic Ca2+ signaling during the development of hypertrophy and heart failure, Circulation 130 (3) (2014) 244–255. [PubMed: 24928680]

[18]. Marrouche NF, et al., Catheter ablation for atrial fibrillation with heart failure, N. Engl. J. Med 378 (5) (2018) 417–427. [PubMed: 29385358]

[19]. Mahajan R, et al., Electrophysiological, Electroanatomical, and structural remodeling of the atria as consequences of sustained obesity, J. Am. Coll. Cardiol 66 (1) (2015) 1–11. [PubMed: 26139051]

[20]. Hohendanner F, et al., Extent and magnitude of low-voltage areas assessed by ultra-high-density electroanatomical mapping correlate with left atrial function, Int. J. Cardiol 272 (2018) 108–112. [PubMed: 30017527]

[21]. Gasparovic H, et al., Atrial apoptosis and fibrosis adversely affect atrial conduit, reservoir and contractile functions, Interact. Cardiovasc. Thorac. Surg 19 (2) (2014) 223–230 (discussion 230). [PubMed: 24722519]

[22]. Khan A, et al., The cardiac atria are chambers of active remodeling and dynamic collagen turnover during evolving heart failure, J. Am. Coll. Cardiol 43 (1) (2004) 68–76. [PubMed: 14715186]

[23]. Tao A, et al., Cardiomyocyte-fibroblast interaction contributes to diabetic cardiomyopathy in mice: role of HMGB1/TLR4/IL-33 axis, Biochim. Biophys. Acta 1852 (10 Pt A) (2015) 2075–2085. [PubMed: 26209013]

[24]. Kang M, Walker JW, Endothelin-1 and PKC induce positive inotropy without affecting pHi in ventricular myocytes, Exp Biol Med (Maywood) 231 (6) (2006) 865–870. [PubMed: 16741014]

[25]. Li X, et al., Endothelin-1-induced arrhythmogenic Ca2+ signaling is abolished in atrial myocytes of inositol-1,4,5-trisphosphate(IP3)-receptor type 2-deficient mice, Circ. Res 96 (12) (2005) 1274–1281. [PubMed: 15933266]

[26]. Gustafsson T, et al., Elevations of local intravascular pressures release vasoactive substances in humans, Clin. Physiol. Funct. Imaging 33 (1) (2013) 38–44. [PubMed: 23216764]

[27]. Wermuth PJ, et al., Stimulation of transforming growth factor-beta1-induced endothelial-to-mesenchymal transition and tissue fibrosis by Endothelin-1 (ET-1): a novel Profibrotic effect of ET-1, PLoS One 11 (9) (2016) e0161988. [PubMed: 27583804]

[28]. Hohendanner F, et al., Inositol-1,4,5-trisphosphate induced Ca2+ release and excitation-contraction coupling in atrial myocytes from normal and failing hearts, J. Physiol 593 (6) (2015) 1459–1477. [PubMed: 25416623]

[29]. Ibrahim M, et al., Cardiomyocyte Ca2+ handling and structure is regulated by degree and duration of mechanical load variation, J. Cell. Mol. Med 16 (12) (2012) 2910–2918. [PubMed: 22862818]

[30]. Herum KM, et al., Mechanical regulation of cardiac fibroblast profibrotic phenotypes, Mol. Biol. Cell 28 (14) (2017) 1871–1882. [PubMed: 28468977]

[31]. Wang J, et al., Mechanical force regulation of myofibroblast differentiation in cardiac fibroblasts, Am. J. Physiol. Heart Circ. Physiol 285 (5) (2003) H1871–H1881. [PubMed: 12842814]

[32]. Yu X, Kennedy RH, Liu SJ, JAK2/STAT3, not ERK½, mediates interleukin-6induced activation of inducible nitric-oxide synthase and decrease in contractility of adult ventricular myocytes, J. Biol. Chem 278 (18) (2003) 16304–16309. [PubMed: 12595539]

[33]. MacKenna D, Summerour SR, Villarreal FJ, Role of mechanical factors in modulating cardiac fibroblast function and extracellular matrix synthesis, Cardiovasc. Res 46 (2) (2000) 257–263. [PubMed: 10773229]

[34]. McMurray JJ, et al., Plasma endothelin in chronic heart failure, Circulation 85 (4) (1992) 1374–1379. [PubMed: 1532540]

[35]. Mayyas F, et al., Association of left atrial endothelin-1 with atrial rhythm, size, and fibrosis in patients with structural heart disease, Circ. Arrhythm. Electrophysiol 3 (4) (2010) 369–379. [PubMed: 20495015]

[36]. Pluteanu F, et al., Progressive impairment of atrial myocyte function during left ventricular hypertrophy and heart failure, J. Mol. Cell. Cardiol 114 (2018) 253–263. [PubMed: 29191788]

[37]. Lau DH, et al., Characterization of cardiac remodeling in a large animal “onekidney, one-clip” hypertensive model, Blood Press. 19 (2) (2010) 119–125. [PubMed: 20367547]

[38]. Eisner DA, et al., Physiological and pathological modulation of ryanodine receptor function in cardiac muscle, Cell Calcium 35 (6) (2004) 583–589 [PubMed: 15110148]

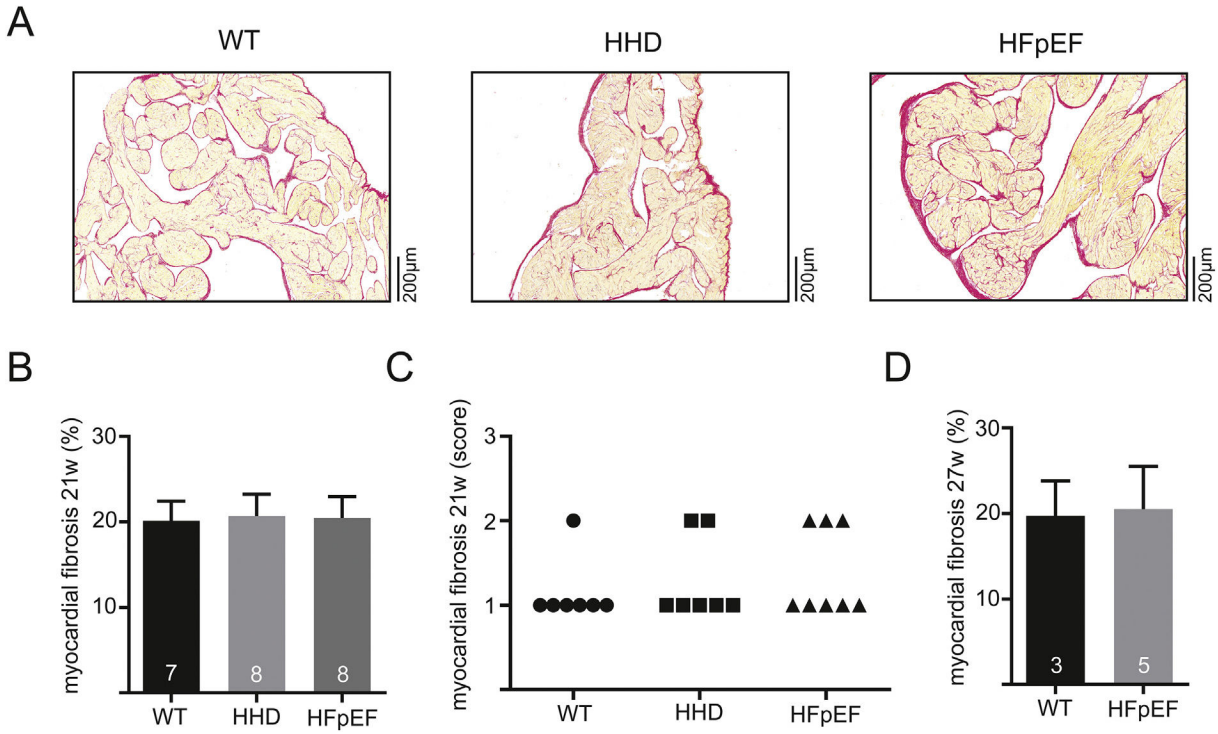

Fig. 1.

Example of histologic sections stained with Picro-Sirius Red dye of the left atrium in 21-week-old WT, HHD and HFpEF (A). Fibrotic tissue is indicated by red color. Total myocardial fibrosis quantified by computer-automated analysis (B) and semi-quantitatively assessed by a blinded expert in veterinary pathology at 21 weeks (C). Computer-automated analysis of myocardial fibrosis at 27 weeks (D). (For interpretation of the references to color in this figure legend, the reader is referred to the web version of this article.)

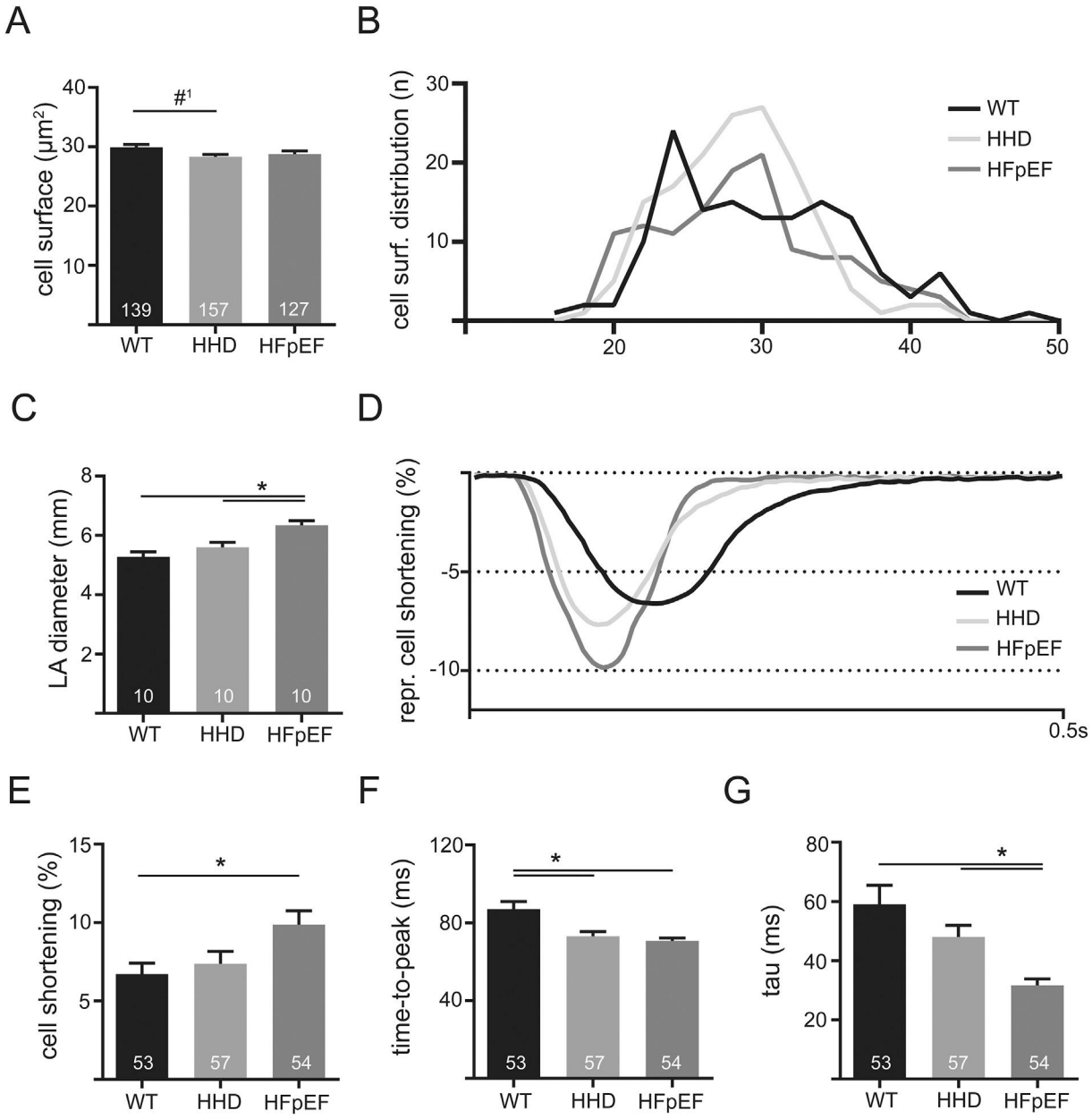

Fig. 2.

Cell surface of LA cardiomyocytes of WT, HHD and HFpEF at 21 weeks (A) and the respective distribution frequency (B). LA diameter derived from transthoracic echocardiography in 21-week-old WT, HHD and HFpEF during diastole (C). Example of contractile function recorded with video edge-detection in 21-week-old WT, HHD and HFpEF at baseline conditions and 1 Hz electrical pacing (D). Cell shortening relative to the size of the cell (E), time to reach maximum amplitude (F) and tau of decay (G). *$p < .05$; #¹p = 0.055.

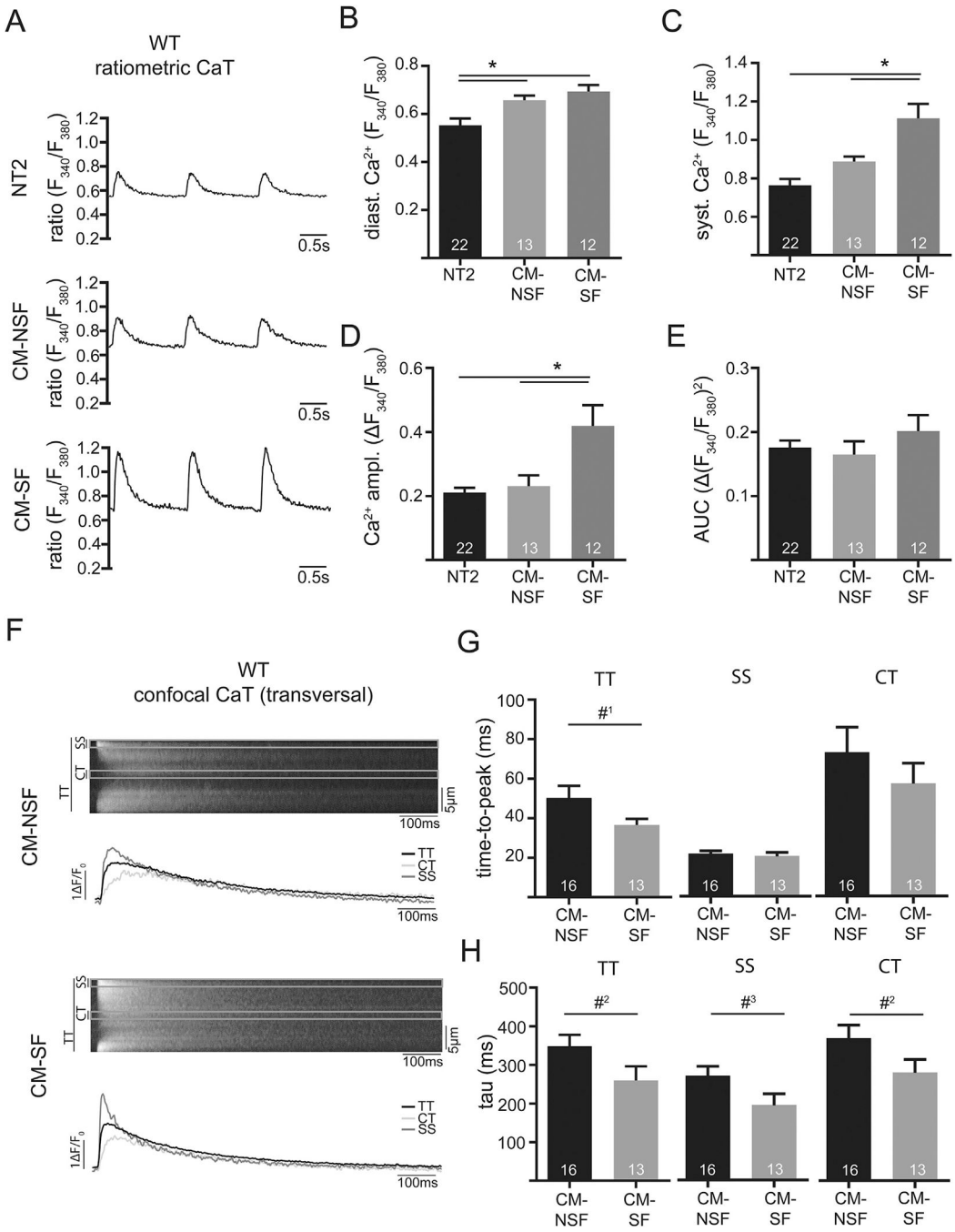

Fig. 3.

Example of ratiometrically recorded CaT (Fura-2) after 1 h incubation with either Normal Tyrode (NT2; 2 mM Ca), conditioned-medium from non-stretched CF (CM-NSF; 0% stretch for 72 h; 1.8 mM Ca) and conditioned medium from stretched CF (CM-SF; 10% stretch for 72 h; 1.8 mM Ca) at 1 Hz steady state stimulation in WT at 21 weeks. Quantification of diastolic (B) and systolic Ca (C), as well as Ca amplitude (D) and area under the curve (E). Example of confocal CaT (Fluo-4) after 1 h incubation with CM-NSF and CM-SF at 1 Hz steady state stimulation. Markings indicate the sub-sarcolemmal region (SS; ROI: 1 µm

below cell surface), central region (CT; ROI: 1 μm in cell center) and the total transverse line scan (TT). Quantification of cellular (TT) and sub-cellular (CT, SS) CaT time-to-peak (G) and tau of decay (H). *$p < .05$; #[1]$p = 0.08$; #[2]$p = 0.07$; #[3]$p = 0.06$.

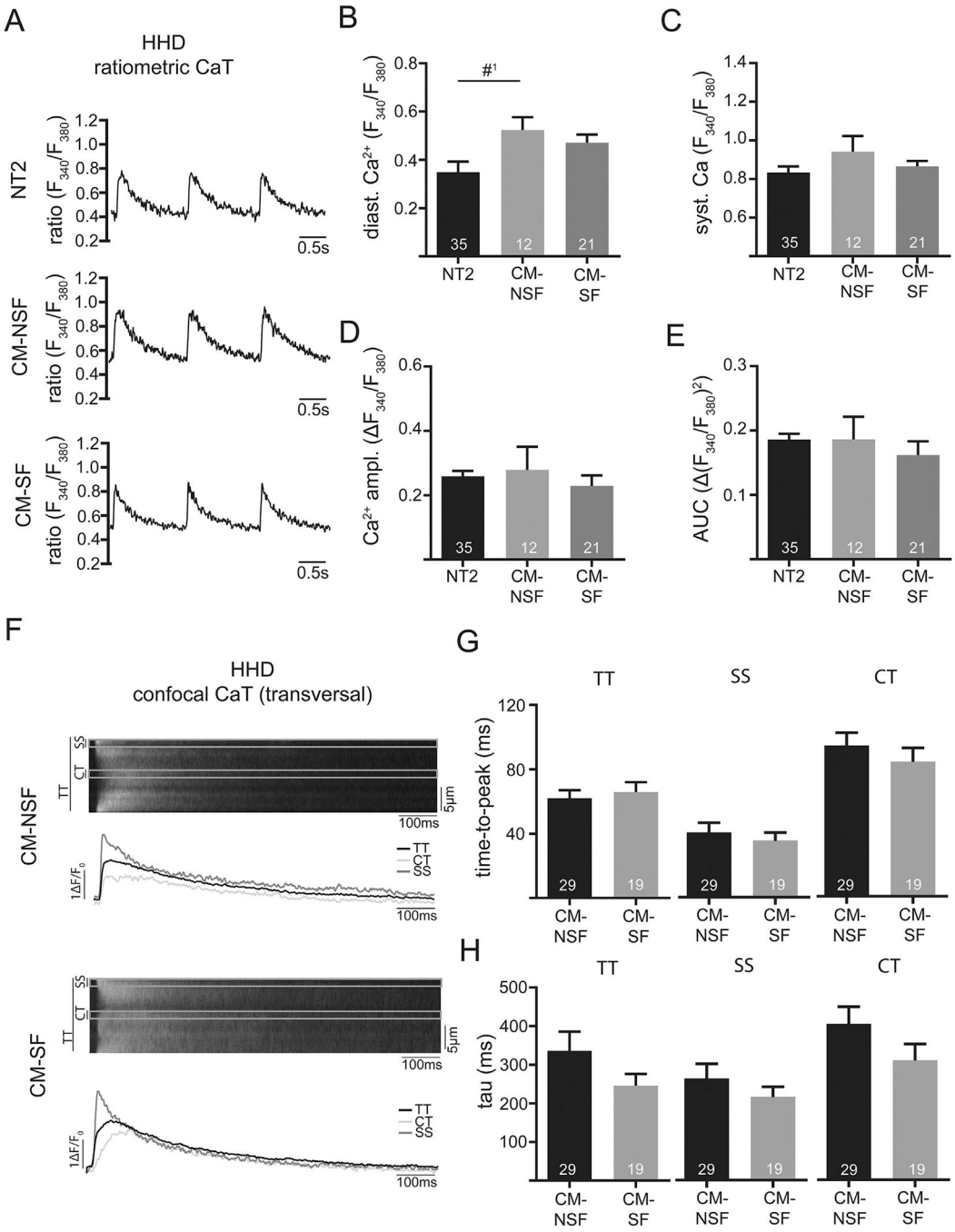

Fig. 4.

Example of ratiometrically recorded CaT (Fura-2) after 1 h incubation with either Normal Tyrode (NT2; 2 mM Ca), conditioned-medium from non-stretched CF (CM-NSF; 0% stretch for 72 h; 1.8 mM Ca) and conditioned medium from stretched CF (CM-SF; 10% stretch for 72 h; 1.8 mM Ca) at 1 Hz steady state stimulation in HHD at 21 weeks. Quantification of diastolic (B) and systolic Ca (C), as well as Ca amplitude (D) and area under the curve (E). Example of confocal CaT (Fluo-4) after 1 h incubation with CM-NSF and CM-SF at 1 Hz steady state stimulation. Markings indicate the sub-sarcolemmal region (SS; ROI: 1 µm

below cell surface), central region (CT; ROI: 1 μm in cell center) and the total transverse line scan (TT). Quantification of cellular (TT) and sub-cellular (CT, SS) CaT time-to-peak (G) and tau of decay (H). $\#^1p = 0.07$.

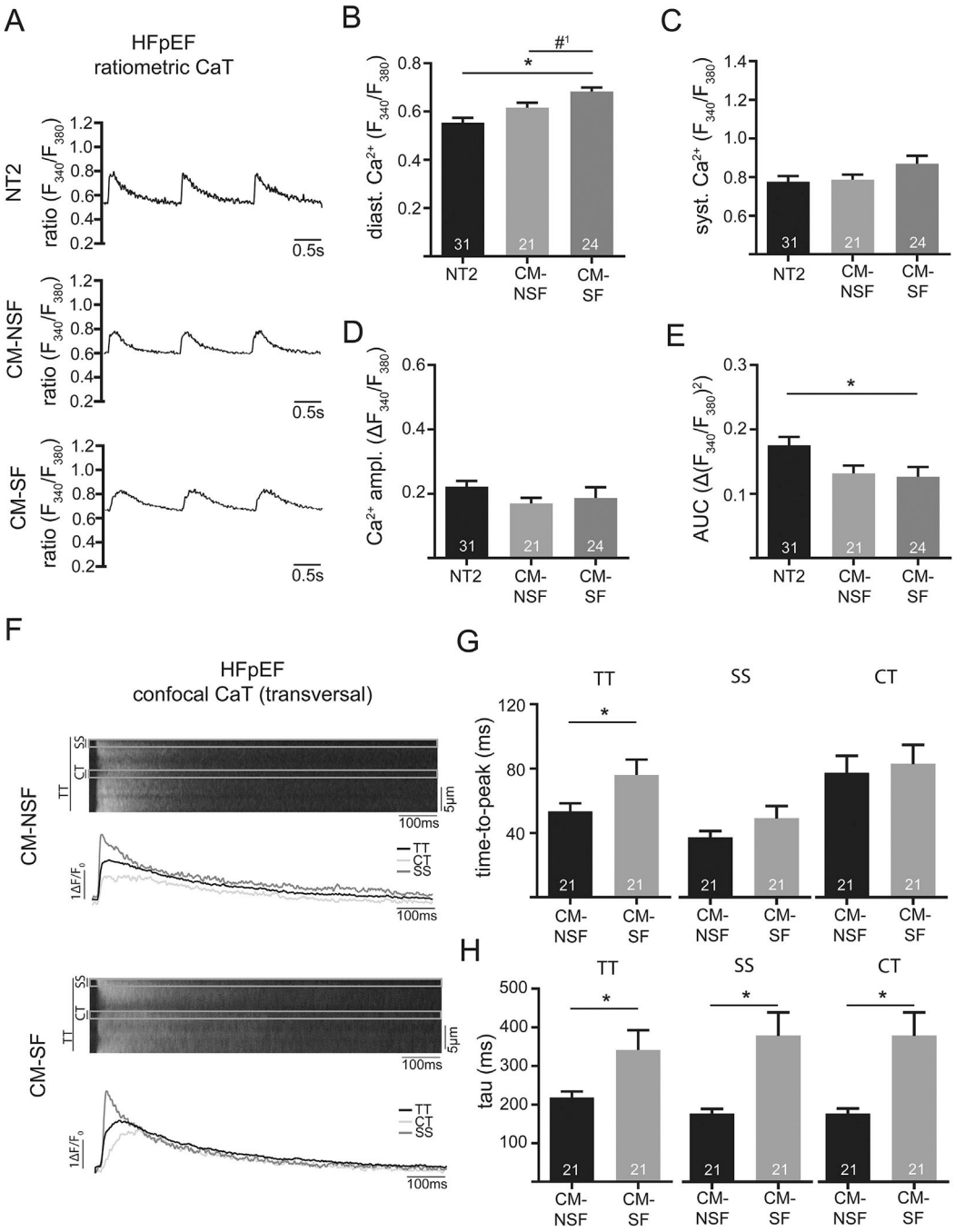

Fig. 5.

Example of ratiometrically recorded CaT (Fura-2) after 1 h incubation with either Normal Tyrode (NT2; 2 mM Ca), conditioned-medium from non-stretched CF (CM-NSF; 0% stretch for 72 h; 1.8 mM Ca) and conditioned medium from stretched CF (CM-SF; 10% stretch for 72 h; 1.8 mM Ca) at 1 Hz steady state stimulation in HFpEF at 21 weeks. Quantification of diastolic (B) and systolic Ca (C), as well as Ca amplitude (D) and area under the curve (E). Example of confocal CaT (Fluo-4) after 1 h incubation with CM-NSF and CM-SF at 1 Hz steady state stimulation. Markings indicate the sub-sarcolemmal region (SS; ROI: 1 µm

below cell surface), central region (CT; ROI: 1 μm in cell center) and the total transverse line scan (TT). Quantification of cellular (TT) and sub-cellular (CT, SS) CaT time-to-peak (G) and tau of decay (H). *$p < .05$; #[1]p =0.07.

A

WT

	CM-NSF	CM-SF
ET-1	51.8	71.3
IL-1β	<31.3	<31.3
IL-6	298	232.6
IL-10	<31.3	89.1
IL-33	<31.3	<31.3
PDGF	<31.3	<31.3
TGF-β	<31.3	<31.3
TNF-α	<12.5	<12.5

pg/ml

B

HHD

	CM-NSF	CM-SF
ET-1	9.1	15.2
IL-1β	<31.3	<31.3
IL-6	<31.3	142.2
IL-10	<31.3	148.1
IL-33	<31.3	<31.3
PDGF	<31.3	<31.3
TGF-β	<31.3	<31.3
TNF-α	<12.5	<12.5

pg/ml

C

HFpEF

	CM-NSF	CM-SF
ET-1	15	15.7
IL-1β	<31.3	<31.3
IL-6	<31.3	<31.3
IL-10	<31.3	<31.3
IL-33	<31.3	<31.3
PDGF	<31.3	<31.3
TGF-β	<31.3	<31.3
TNF-α	<12.5	<12.5

pg/ml

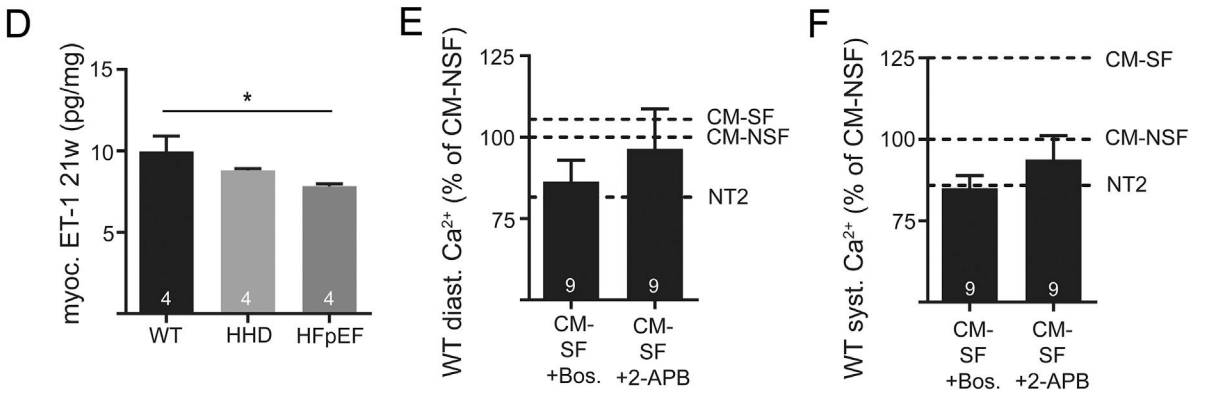

Fig. 6.

Quantification of selected cytokines in CM-NSF and CM-SF in WT (A), HHD (B) and HFpEF (C) at 21 weeks. Myocardial tissue levels of ET-1 in the left atrium (D). Diastolic (E) and systolic Ca (F) after 1 h incubation with CM-SF in the presence of ET-1 receptor antagonist Bosentan or IP_3 receptor inhibitor 2-APB. Reference for CM-SF (with or without Bosentan/2-APB) was obtained in two different sets of experiments with $n = 13$ and $n = 11$ CM-NSF cells. Dashed lines indicate respective Ca levels after treatment with NT2, CM-NSF and CM-SF without Bosentan/2-APB. *$p < .05$.

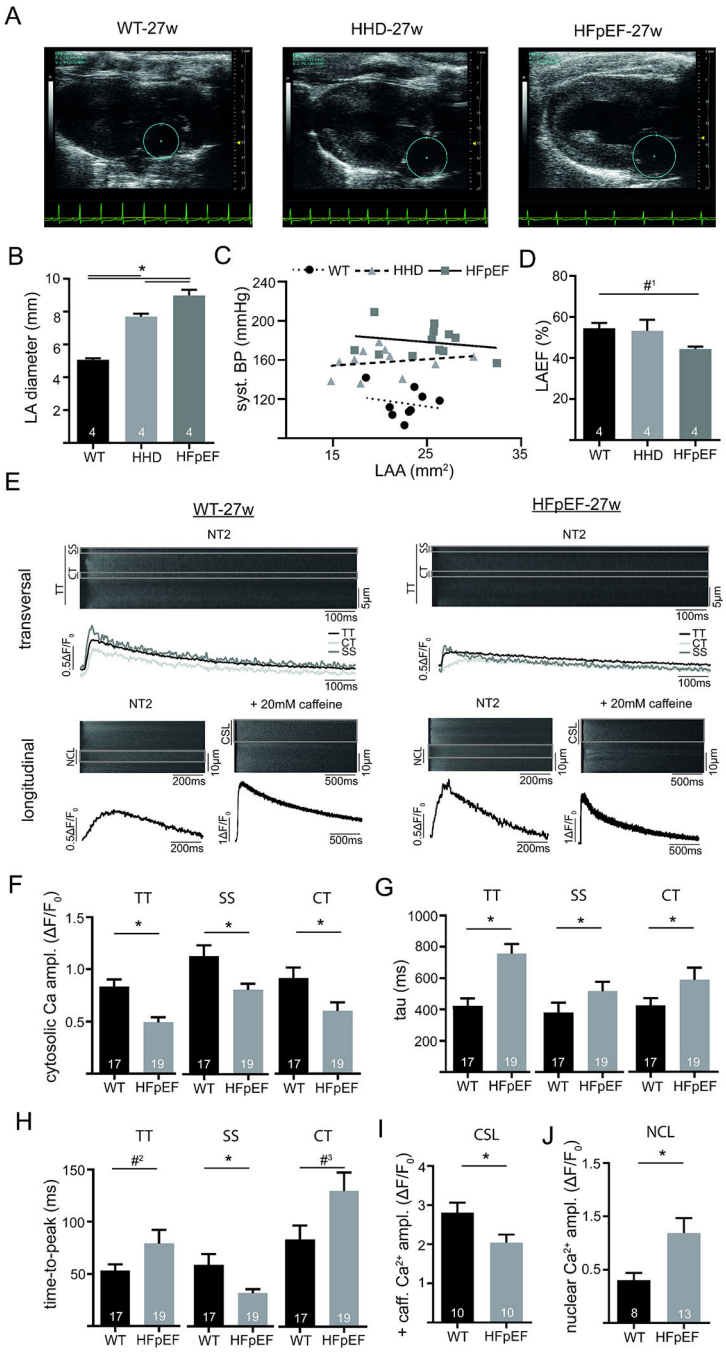

Fig. 7.

In vivo atrial function in a model of advanced atrial remodeling. Example of parasternal longitudinal axis images obtained with echocardiography in WT, HHD and HFpEF at 27 weeks (A). Marked area depicts the left atrium. LA diameter during diastole (B) and LA ejection fraction (D). Correlation of systolic blood pressure (invasive catheterization) with LA area (C). Example of confocally recorded transversal and longitudinal CaT (E; Fluo4) at baseline conditions in 27-week-old WT and HFpEF at 1 Hz steady state stimulation (transversal and longitudinal) and application of caffeine (longitudinal; 20 mM; without

electric stimulation). Markings in the transversal line scans indicate the sub-sarcolemmal region (SS; ROI: 1 μm below cell surface), central region (CT; ROI: 1 μm in cell center) and the total line scan (TT), while markings in the longitudinal line scans indicate the cytosolic region between the sarcolemma and nucleus (CSL) and the nucleus (NCL). Cytosolic (TT) and subcellular (SS, CT) Ca amplitude (F), tau of decay (G) and time-to-peak (H) at 1 Hz steady state stimulation in NT2. Caffeine-triggered (20 mM) cytosolic Ca release without electrical stimulation (I). Nuclear Ca amplitude at 1 Hz steady state stimulation (J). *$p < .05$; #$^{1}p = 0.21$; #$^{2} = 0.09$; #$^{3}p = 0.051$.

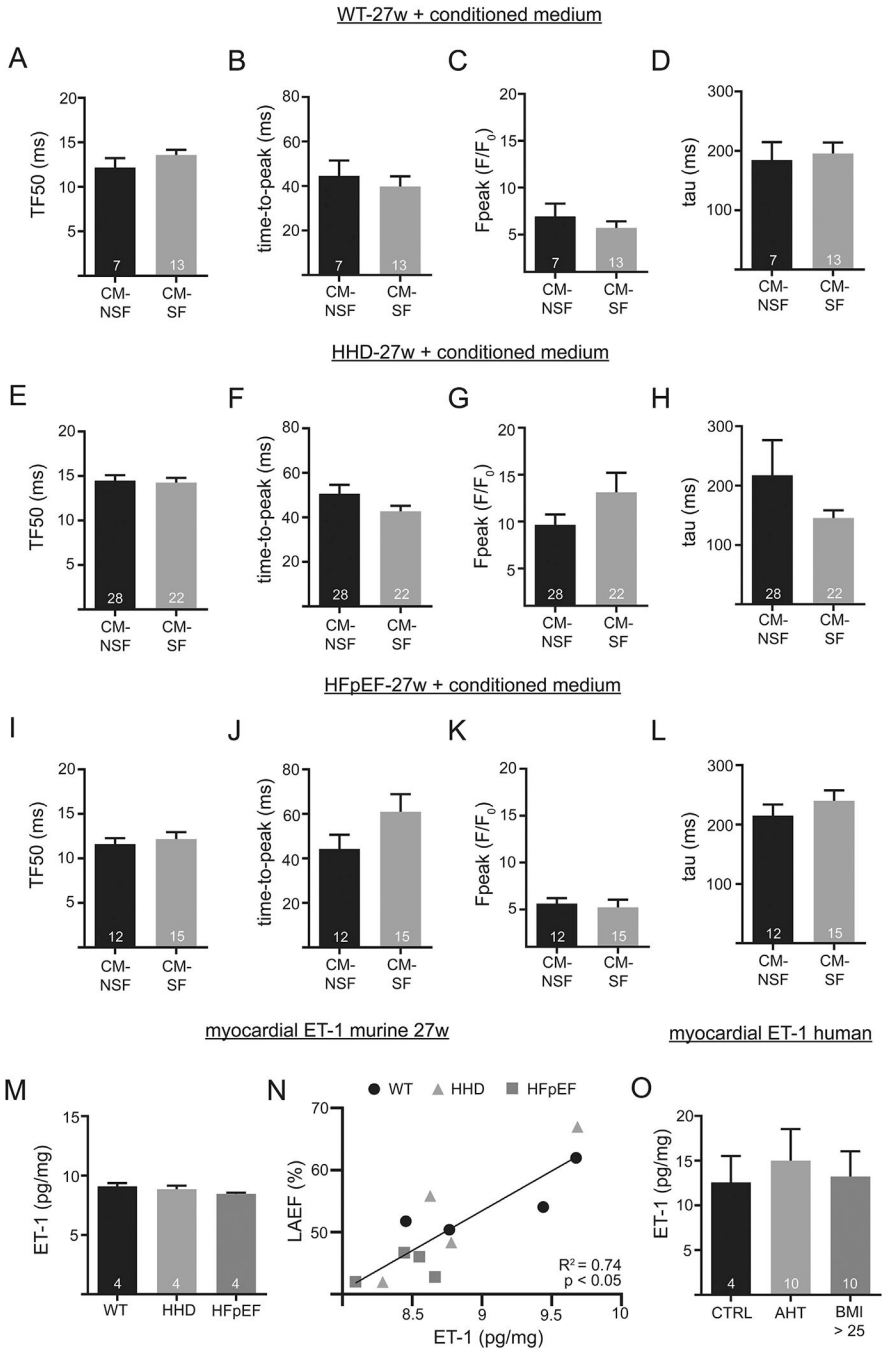

Fig. 8.

Confocal Ca imaging in 27-week-old animals after 1 h incubation with CM-NSF and CM-SF from 21-week-old animals. Transversal line scans at 1 Hz steady state stimulation. TF50, time-to-peak, Ca peak, and tau of decay of WT (A-D), HHD (*E*-H) and HFpEF (I-L). Myocardial tissue levels of ET-1 in the left atrium at 27 weeks (M). Correlation of LA ejection fraction and myocardial ET-1 (N). Myocardial tissue levels of ET-1 in a cohort of

patients (O). The control group is represented by patients with a BMI ≤ 25 and no history of AHT.